

Evidence for two superconducting energy gaps in MgB₂ by point-contact spectroscopy

P. Szabó^{*,§}, P. Samuely^{*}, J. Kacmarčík^{*},
Th. Klein[§], J. Marcus[§], D. Fruchart[‡],
S. Miraglia[‡], C. Marcenat[°], & A.G.M. Jansen[§]

^{*}Institute of Experimental Physics, Slovak Academy of Sciences, SK-04353 Kosice, Slovakia

[§]Laboratoire d'Etudes des Propriétés Electroniques des Solides, Centre National de la Recherche Scientifique, B.P. 166, F-38042 Grenoble Cedex 9, France.

[‡]Laboratoire de Cristallographie, BP 166, 38042 Grenoble Cedex 9, France

[°]CEA-Grenoble, Département de Recherche Fondamentale sur la Matière Condensée, 17 rue des Martyrs, 38054 Grenoble Cedex 9, France

[§]Grenoble High Magnetic Field Laboratory, Max-Planck-Institut für Festkörperforschung and Centre National de la Recherche Scientifique, B.P. 166, F-38042 Grenoble Cedex 9, France.

Two decades of the boom in the field of superconductivity has recently been boosted by the surprising discovery of superconductivity in MgB₂¹. In contrast to the cuprates, the first tunneling^{2,4} and point-contact^{5,6} spectroscopy measurements have unequivocally shown that this system is a *s*-wave superconductor and isotope effects^{7,8} have pointed towards a phonon mechanism. However, the size of the superconducting energy gap has remained unclear. We report here on strong experimental support for the multiband model of superconductivity recently proposed by Liu *et al.*⁹ thus showing that MgB₂ belongs to an original class of superconductors in which two distinct 2D and 3D Fermi surfaces contribute to superconductivity. Indeed, our point-contact spectroscopy experiments clearly show the existence of two distinct superconducting gaps with $D_S(0) = 2.8$ meV and $D_L(0) = 7$ meV. Both gaps close near to the bulk transition temperature $T_c = 39$ K. Our measurements in magnetic field show directly in the raw data the presence of two superconducting gaps at all temperatures up to the same bulk transition T_c pointing that the two gaps are inherent to the superconductivity in MgB₂.

Although quite scattered, the first spectroscopy measurements^{2-6,10} yielded to superconducting gap values surprisingly smaller than the BCS weak coupling limit $2D/k_B T_c = 3.52$. Moreover simultaneous topographic imaging and quasiparticle density of states mapping¹¹ revealed substantial inhomogeneities

at the surface of the sample as well as a large scattering of the energy gap values measured at different parts of the polycrystalline sample (with D ranging from 3 to 7.5 meV). This energy gap distribution can be caused by sample inhomogeneities. However, Giubileo *et al.*¹¹ also observed a *superposition* of two gaps ($D_S(0) = 3.9$ meV and $D_L(0) = 7.5$ meV) in some of their local tunneling spectra. The same inhomogeneity argument could of course also explain such a superposition but a much more attractive scenario would be a two-gap model. Such a model has been first developed by Suhl *et al.*¹² in the case of overlapping *s*- and *d*- bands in conventional superconductors (such as V, Nb, Ta). Experimental evidence for the existence of two band superconductivity was obtained by tunneling spectroscopy in Nb-doped SrTiO₃¹³. A similar model has been recently proposed by Liu *et al.*⁹ for MgB₂. It is here based on the coexistence of a two-dimensional Fermi surface ($p_{x,y}$ orbitals) perpendicular to the *z* direction and a three dimensional (p_z bonding and antibonding bands) one. This model is then predicting the existence of two different energy gaps being respectively smaller (for the 3D gap) and slightly larger (for the 2D gap) than the expected weak coupling value.

Indications for the existence of two gaps in MgB₂ have also been found in specific heat measurements^{14,15} and low temperature Raman-scattering¹⁶ experiments reveal two peaks for two different gaps. However, it is still necessary to show that these two gaps *coexist up to T_c* in order to validate this scenario. We show here direct and clear evidence for this coexistence using point-contact spectroscopy in a magnetic field.

Blonder, Tinkham and Klapwijk (BTK) have developed a theory¹⁷ describing the electrical transport in ballistic contacts between a normal (N) and a superconducting (S) electrode with different possible interfaces between them: from a pure conducting interface where the Andreev reflection dominates up to the well known insulating barrier (i.e. the Giaever tunneling case). The most important consequence of this theory is that *any* point contact geometry will be able to provide a direct spectroscopic information about the superconducting energy gap. In the pure Andreev limit, if a quasi-particle is accelerated by an applied voltage V such that $V < D/e$, a direct transfer to the superconducting electrode is forbidden and a hole is then retro-reflected in the normal electrode in order to allow the formation of a Cooper pair in the superconductor. The overall current (and differential conductance $S = dI/dV$) for $V < D/e$ is then twice higher than the value for $V > D/e$. In the intermediate case a dip appears for $V = 0$. Two peaks are then visible at $V \sim \pm D/e$. The evolution of the dI/dV vs. V curves for different interfaces characterised with the barrier strength Z is schematically presented in Figure 1a. Note that, as shown by Deutscher¹⁸, the Giaever-like tunneling spectroscopy will provide the single

particle excitation energy (i.e. the energy required to break the Cooper pairs required for superconductivity) whereas the Andreev reflection is associated with the energy range of coherence in the superconducting state. If both methods yield to similar values in conventional superconductors they led to very different energy gaps in underdoped high- T_c oxides. As the point-contact geometry directly probes the coherence of the superconducting state, it is probably the most adapted technique to determine the superconducting energy gap. Another advantage of point-contact spectroscopy is that the normal electrode is pushed into the sample in order to probe a clean surface.

Point-contact measurements have been performed on polycrystalline MgB_2 samples with $T_c \sim 39$ K. A special point-contact approaching system with a negligible thermal expansion allows for the temperature and magnetic field measurements up to T_c . The point contacts were stable enough to be measured in the magnetic field of a superconducting coil. A standard lock-in technique at 400 Hz was used to measure the differential resistance as a function of applied voltage on the point contacts. The microconstrictions were prepared by pressing a copper tip (formed by electrochemical etching) on the freshly polished surface of the superconductor. MgB_2 samples were prepared from boron powder (99,5 % pure, Ventron) and magnesium powder (98% Mg + 2 % KCl, MCP Techn.), in relative proportion 1.05 : 2. A 2 g mass of the mixed powders was introduced into a tantalum tube, then sealed by arc melting under argon atmosphere (purity 5N5). The tantalum ampoule was heated by high frequency induction at 950°C for about 3 hours. After cooling down to room temperature, the sample was analysed by X-ray diffraction and Scanning Electron Microscope. Among the brittle dark grey MgB_2 powder (grain size < 20 μm), a few hard but larger grains (0.1 to 1 mm) were found. Laue patterns show evidence for only a limited number of single crystals in each grain. Resistivity and a.c. susceptibility measurements of these larger grains reveal particularly abrupt transition ($\Delta T_c \sim 0.6$ K) indicating their high quality in comparison with that of the fine powder.

Figure 1b shows typical examples of the *conductance versus voltage* spectra obtained for the various Cu- MgB_2 junctions with different barrier transparencies. All shown point-contact conductances have been normalized to the value at the high-voltage bias. The spectrum had a more tunneling-like character when the tip first touched the surface (i.e. with a barrier resistance $R \sim 100 \Omega$) and then continuously transformed into a form with a direct conductance as the tip was pushed into the sample (down to $R \sim 6 \Omega$). Almost all curves reveal a two-gap structure where the smaller gap maxima are displayed at around 2.8 mV and the large gap maxima at about 7 mV, placed symmetrically around the zero bias. Even, if in some cases only the smaller gap is apparent (as

shown in the lowest curve of Figure 1b), its width is hiding a contribution of the second gap. Then, as we show below, a magnetic field can suppress the smaller gap and the large one will definitely emerge. All our curves could be fitted by the sum of the two BTK conductances $a s_L + (1-a) s_S$ with the weight factor a varying from $\sim 10\%$ to $\sim 90\%$ depending on the position of the tip (this scattering of the a value is probably related to different crystallographic orientations at the different microconstrictions). We thus definitely observed two distributions with the smaller gap scattered around 2.8 meV and the second one around 7 meV.

As pointed out above, the smaller gap could be caused by a weakening of the superconducting state. That is why it is important to show that it still exists at high temperatures in order to validate the two-gap scenario with one single critical temperature. The temperature dependencies of the point-contact spectra have been examined on five different samples in about 10 spectra with a clear two-gap structure. Due to thermal smearing, the two well resolved peaks in the spectrum merge together as the temperature increases. Consequently, the presence of two gaps is not so evident in the raw data (see Figure 2a). However the data could be well fitted at all temperatures by the sum of two BTK contributions with the transparency coefficient Z and the weight factor a kept constant and without any parallel leakage conductance. The point-contact conductances of one spectrum at different temperatures are shown in Figure 2a together with the corresponding BTK fits. The resulting energy gaps D_L and D_S together with those obtained for two other point contacts with different weight values a are shown in Figure 2b.

Since it is evident from Figure 2b that both gaps are closing near the same bulk transition temperature, our data give experimental support for the two gap model. In the classical BCS theory, an energy gap with $D_S = 2.8$ meV could not exist for a system with T_c above $2D/3.5k_B \sim 19$ K. Moreover, we obtained a very weakly coupled gap with $2D_S/k_B T_c \approx 1.7$ and a strongly coupled gap with $2D_L/k_B T_c \approx 4.1$ in very good agreement with the predictions of Liu *et al.*⁹ (a 3D gap ratio $2D_S/k_B T_c \approx 1.3$ and a 2D gap ratio $2D_L/k_B T_c \approx 4.0$). The temperature dependencies are in a good agreement with the prediction of the BCS theory. Small deviations from this theory have been predicted by Liu *et al.*⁹ but these deviations are within our error bars for the large gap D_L while in the case of the small gap D_S there is a tendency for more rapid closing at higher temperatures near to T_c (see Figure 2b) as expected theoretically⁹.

Even much stronger evidence for the inherent presence of two gaps in the superconductivity of MgB_2 is obtained by our magnetic field measurements. Figure 3 displays the effect of the magnetic field up to 1 Tesla on the two gaps measured at four different temperatures. At $T = 4.2$ K the two gaps are clearly visible for zero magnetic field $H = 0$

but the peaks corresponding to the small gap are rapidly affected by a magnetic field. The contribution of this small gap almost completely disappears at 1 T whereas the large gap still remains clearly visible. The other sets of spectra have been recorded at 10, 20 and 30 K. As already shown in Figure 2a, the spectra are so smeared out above 20 K that the presence of the two gaps is not clearly visible and we have to rely on the fitting procedure. On the contrary, nothing like this holds when we apply the magnetic field. Indeed, as the smaller gap is rapidly suppressed by the field, so is its contribution to the overall point-contact conductance. As clearly visible at 4.2K and 10K, this suppression leads to the formation of a deep broad minimum in the conductance at zero bias with increasing magnetic field. Similarly, at 20K and 30K the peaks corresponding to the large gap become much *better resolved in a magnetic field*. This could not happen if there was not a contribution of the small gap in the zero-field point-contact conductance at these elevated temperatures. Indeed, a one-gap spectrum would only smear out with increasing magnetic field due to pair-breaking effect. This effect thus unambiguously shows that the two gaps coexist up to T_c , thus confirming the two band model of superconductivity in MgB_2 .

The specific heat measurements performed by Bouquet *et al.*¹⁴ revealed a strong reduction of the electronic density of states at low temperatures suggesting the presence of a second small energy gap which, in striking similarity with our direct observations, could be suppressed by a ~ 1 Tesla magnetic field. Specific heat is a bulk thermodynamic quantity and the excellent consistency of these measurements with our spectroscopic results further demonstrates that the existence of these two gaps is an intrinsic property of MgB_2 . Indirect observations of two gaps were also obtained from the temperature dependence of the specific heat in the conventional superconductors Nb, Ta and V¹⁹ but to the best of our knowledge, a clear and direct observation for the presence of two gaps existing up to the same T_c was never observed before by spectroscopic measurements. The possibility that these two gaps have different dimensionalities makes this system particularly attractive for further studies.

References

1. Nagamatsu, J., Nakagawa, N., Muranaka, T., Zenitani, Y. & Akimitsu, J. Superconductivity at 39 K in magnesium diboride. *Nature* **410**, 63-64 (2001).
2. Rubio-Bollinger, G., Suderow, H., Vieira, S. Tunneling spectroscopy in small grains of superconducting MgB_2 . Preprint cond-mat/0102242 at <<http://xxx.lanl.gov>> (2001).
3. Karapetrov, G., Iavarone, M., Kwok, W.K., Crabtree, G.W., & Hinks, D.G. Scanning Tunneling Spectroscopy in MgB_2 . *Phys. Rev. Lett.* **86**, 4374-4277 (2001).
4. Schmidt, H., Zasadzinski, J.F., Gray, K.E., & Hinks, D.G. Energy Gap from Tunneling and Metallic Sharvin Contacts onto MgB_2 : Evidence for a Weakened Surface Layer. Preprint cond-mat/0102389 at <<http://xxx.lanl.gov>> (2001).
5. Kohen, A., & Deutscher, G. Symmetry and Temperature dependence of the Order parameter in MgB_2 from point contact measurements. Preprint cond-mat/0103512 at <<http://xxx.lanl.gov>> (2001).
6. Plecenik, A., Benacka, S., Kus, P., & Grajcar, M. Superconducting gap parameters of MgB_2 obtained on MgB_2/Ag and MgB_2/In junctions. Preprint cond-mat/0104038 at <<http://xxx.lanl.gov>> (2001).
7. Bud'ko, S.L., Lapertot, G., Petrovic, C., Cunningham, C.E., Anderson, N., & Canfield, P.C. Boron Isotope Effect in Superconducting MgB_2 . *Phys. Rev. Lett.* **86**, 1877-1879 (2001).
8. Hinks, D.G., Claus, H., Jorgensen, J.D. The complex nature of superconductivity in MgB_2 as revealed by the reduced total isotope effect. *Nature*, **411**, 457-461 (2001).
9. Liu, Amy Y., Mazin, I.I., & Kortus, J. Beyond Eliashberg superconductivity in MgB_2 : anharmonicity, two-phonon scattering, and multiple gaps. Preprint cond-mat/0103570 at <<http://xxx.lanl.gov>> (2001); Kortus, J., Mazin, I.I. Belashenko, K.D., Antropov, V.P., Boyer, L.L. Superconductivity of metallic boron in MgB_2 . cond-mat/0101446 at <<http://xxx.lanl.gov>> (2001).
10. Takahashi, T., Sato, T., Souma, S., Muranaka T., & Akimitsu, J. High-Resolution Photoemission Study of MgB_2 . Preprint cond-mat/0103079 at <<http://xxx.lanl.gov>> (2001).
11. Giubileo, F., Roditchev, D., Sacks, W., Lamy, R., & Klein, J. Strong Coupling and Double Gap Density of States in Superconducting MgB_2 . Preprint cond-mat/0105146 at <<http://xxx.lanl.gov>> (2001).
12. Suhl, H., Matthias, B.T., & Walker, L.R. Bardeen-Cooper-Schrieffer theory of superconductivity in the case of overlapping bands. *Phys. Rev. Lett.* **3**, 552-554 (1959).
13. Binning, G., Baratoff, A., Hoenig, H.E., Bednorz, J.C. Two band superconductivity in Nb-doped SrTiO_3 *Phys. Rev. Lett.* **45**, 1352-1355 (1980).
14. Bouquet, F., Fisher, R. A., Phillips, N. E., Hinks, D. G., & Jorgensen, J. D. Specific heat of Mg^{11}B_2 . Preprint cond-mat/0104206 at <<http://xxx.lanl.gov>>.
15. Wang, Y., Plackowski, T., & Junod, A. Specific heat in the superconducting and normal state (2-300 K, 0-16 Teslas), and magnetic susceptibility of the 38-K superconductor MgB_2 : evidence for multicomponent gap. *Physica C* **355**, 179 (2001).
16. Chen, X.K., Konstantinovic, M. J., Irwin, J.C., Lawrie, D.D., & Franck, J.P. Evidence for Two Superconducting Gaps in MgB_2 . Preprint cond-

mat/0104005 at <http://xxx.lanl.gov> (2001).

17. Blonder, G.E., Tinkham, M., & Klapwijk, T.M. Transition from metallic to tunneling regimes in superconducting microconstrictions: Excess current, charge imbalance, and supercurrent conversion. *Phys. Rev. B* **25**, 4515-4532 (1982).

18. Deutscher, G. Coherence and single-particle excitations in the high-temperature superconductors. *Nature* **397**, 410-412 (1999).

19. Shen, L.Y.L., Senozan, N.M., & Philips, N.E. Evidence for two energy gaps in high-purity superconducting Nb, Ta, and V. *Phys. Rev. Lett.* **14**, 1025-1028 (1965).

ACKNOWLEDGEMENTS. This work has been supported by the Slovak VEGA grant 1148.

Correspondence and requests for materials should be addressed to P.Sz. (e-mail: pszabo@saske.sk).

Figure captions:

Figure 1a Numerical simulation of the BTK model at different values of the barrier strength Z , representing behavior of the point-contact spectra for $D = 7\text{meV}$ between Giaver tunneling ($Z=10$) and clean Andreev reflexion ($Z = 0$) at $T=4.2\text{K}$. **b**, Experimentally observed evolution of the Cu – MgB_2 point-contact spectra at $T = 4.2\text{ K}$ (full lines). The upper curves are vertically shifted for the clarity. Dotted lines display fitting results for the thermally smeared BTK model with $D_S = 2.8 \pm 0.1\text{ meV}$, $D_L = 6.8 \pm 0.3\text{ meV}$ for different barrier transparencies and weight factors.

Figure 2a Differential conductances of Cu – MgB_2 point-contact measured (full lines) and fitted (dotted lines) for the thermally smeared BTK model at signed temperatures. The fitting parameters $a = 0.71$, $Z = 0.5$ had the same values at all temperatures. **b**, Temperature dependencies of both energy gaps ($D_S(T)$ – solid symbols, $D_L(T)$ - open symbols) determined from the fitting on three different point-contacts are displayed with three corresponding different symbols. $D_S(T)$ and $D_L(T)$ points determined from the same contact are plotted with the same (open and solid) symbols. Full lines represent BCS predictions.

Figure 3a, b, c, d Experimentally observed influence of the applied magnetic field on the two gap structure of the normalized point-contact spectra at indicated temperatures. These spectra clearly reveal that both gaps exists in zero field up to T_c as shown by the rapid suppression of the small gap structure ($D_S = 2.8\text{meV}$) with magnetic field which leads to a broad deep minimum at zero bias.

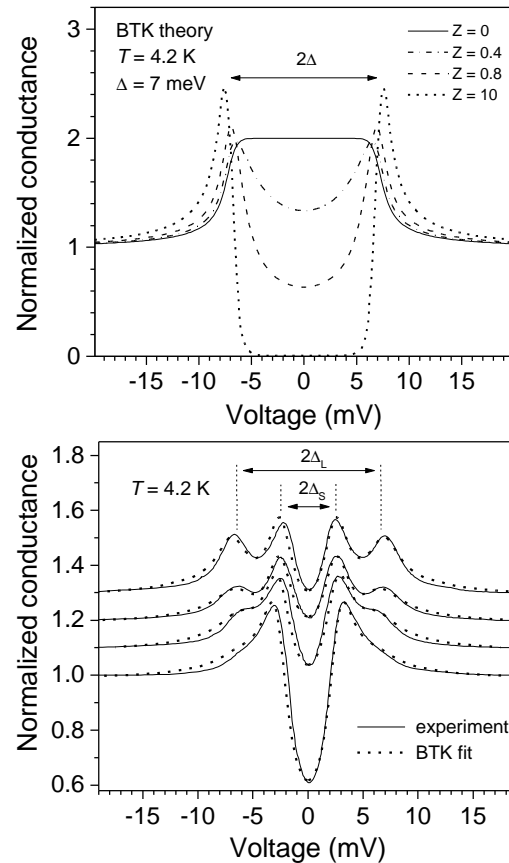


Figure 1a Numerical simulation of the BTK model at different values of the barrier strength Z , representing behavior of the point-contact spectra for $D = 7\text{meV}$ between Giaver tunneling ($Z=10$) and clean Andreev reflexion ($Z = 0$) at $T=4.2\text{K}$. **b**, Experimentally observed evolution of the Cu – MgB_2 point-contact spectra at $T = 4.2\text{ K}$ (full lines). The upper curves are vertically shifted for the clarity. Dotted lines display fitting results for the thermally smeared BTK model with $D_S = 2.8 \pm 0.1\text{ meV}$, $D_L = 6.8 \pm 0.3\text{ meV}$ for different barrier transparencies and weight factors.

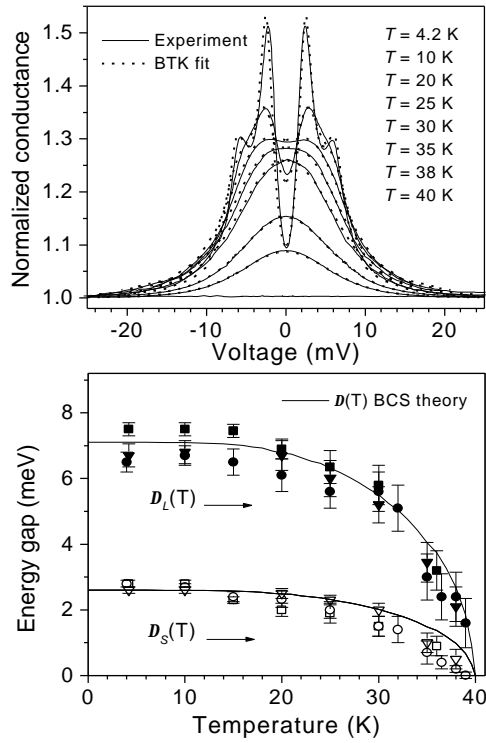


Figure 2a Differential conductances of Cu – MgB₂ point-contact measured (full lines) and fitted (dotted lines) for the thermally smeared BTK model at signed temperatures. The fitting parameters $a = 0.71$, $Z = 0.5$ had the same values at all temperatures. **b**, Temperature dependencies of both energy gaps ($D_S(T)$ – solid symbols, $D_L(T)$ - open symbols) determined from the fitting on three different point-contacts are displayed with three corresponding different symbols. $D_S(T)$ and $D_L(T)$ points determined from the same contact are plotted with the same (open and solid) symbols. Full lines represent BCS predictions.

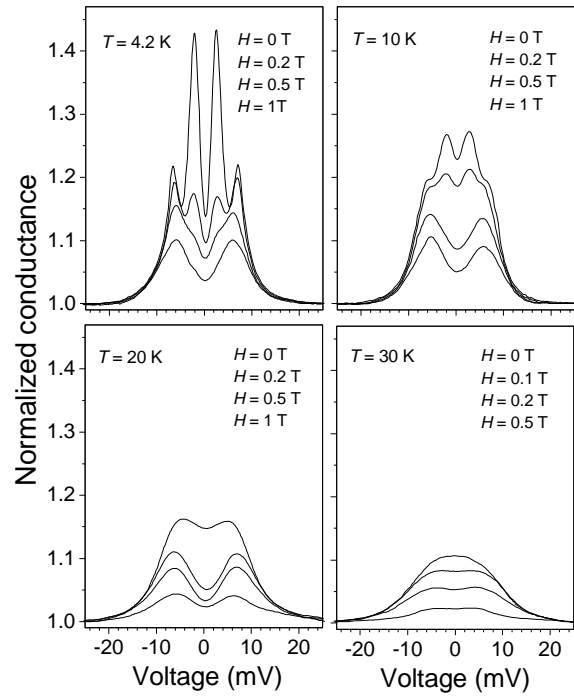


Figure 3a, b, c, d Experimentally observed influence of the applied magnetic field on the two gap structure of the normalized point-contact spectra at indicated temperatures. These spectra clearly reveal that both gaps exist in zero field up to T_c as shown by the rapid suppression of the small gap structure ($D_S = 2.8\text{meV}$) with magnetic field which leads to a broad deep minimum at zero bias.